Variational Simulation of the Hubbard Model using Majorana-based Fermion-to-Qubit Mapping

Ashutosh Tripathi

Department of Theoretical Physics
Tata Institute of Fundamental Research, Mumbai

Monsoon Hadrons 2026
June 24, 2026

Collaborators
Debasish Banerjee   Sandip Maiti   Nilmani Mathur

Motivation

- Variational quantum algorithms provide a promising framework for near-term quantum devices.
- Efficient quantum simulation of fermionic systems remains a major challenge. Two broad approaches exist for fermionic quantum simulations.
- Native fermionic quantum hardware aims to directly encode fermionic statistics.
- Bosonization techniques map fermionic degrees of freedom onto qubits using fermion-to-qubit transformations.
- We study the spinless Hubbard model using the Variational Quantum Eigensolver (VQE) by employing the Derby–Klassen mapping [arXiv:2003.06939].

Variational Quantum Eigensolver

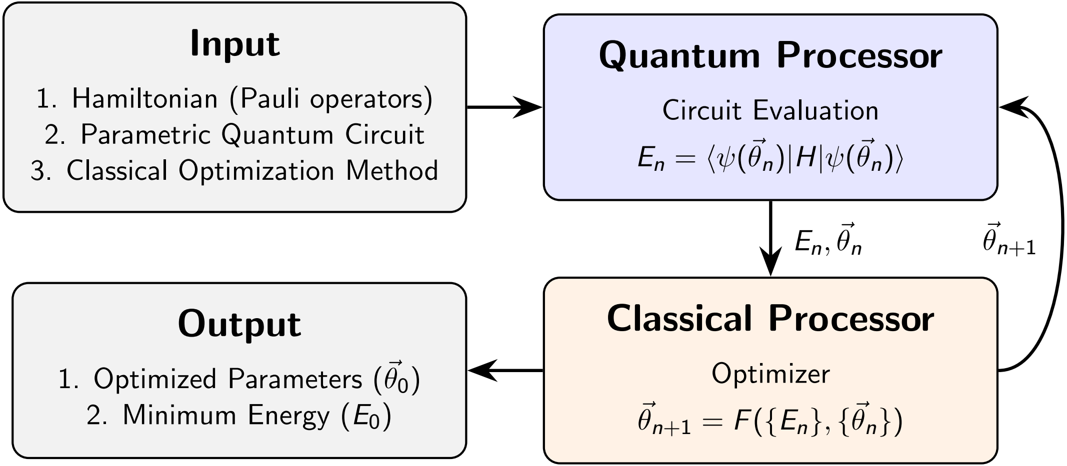

Jordan-Wigner mapping

Anti-commutation relation,

$$\{a_i, a_j\} = 0, \tag{1}$$
$$\{a_i^\dagger, a_j^\dagger\} = 0, \tag{2}$$
$$\{a_i, a_j^\dagger\} = \delta_{ij}. \tag{3}$$

Jordan–Wigner mapping [Eur. Phys. J. A 47, 631 (1928).],

$$a_j = \left(\prod_{k=1}^{j-1} Z_k\right) \frac{X_j + iY_j}{2}, \tag{4}$$
$$a_j^\dagger = \left(\prod_{k=1}^{j-1} Z_k\right) \frac{X_j - iY_j}{2}. \tag{5}$$

- Efficient in 1D.
- Long Pauli strings in 2D.
- More measurements needed.

Derby–Klassen Majorana Mapping

Majorana operators are defined as

$$\bar{\gamma}_k = i(a_k^\dagger - a_k), \quad (6)$$
$$\gamma_k = a_k^\dagger + a_k. \quad (7)$$

Edge and vertex operators:

$$E_{jk} = -i\gamma_j\gamma_k, \quad (8)$$
$$V_j = -i\gamma_j\bar{\gamma}_j. \quad (9)$$

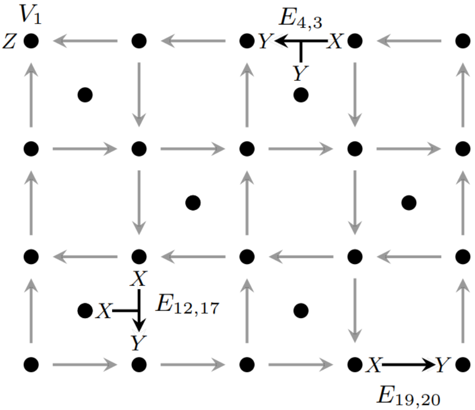

Source: [arXiv:2003.06939]

Advantages

- Preserves locality.
- Suitable for higher-dimensional lattices.

Vertex and Face Qubits

Edge and vertex operators:

$$E_{jk} = -i\gamma_j\gamma_k, \qquad (10)$$
$$V_j = -i\gamma_j\bar{\gamma}_j. \qquad (11)$$

In mapped qubits, the vertex operators become

$$\tilde{V}_j = Z_j. \qquad (12)$$

and the edge operators become

$$\tilde{E}_{jk} = \begin{cases} X_j Y_k X_{F(j,k)}, \\ -X_j Y_k X_{F(j,k)}, \\ X_j Y_k Y_{F(j,k)}, \end{cases} \qquad (13)$$

where $F(j,k)$ denotes the face qubit associated with edge (j,k).

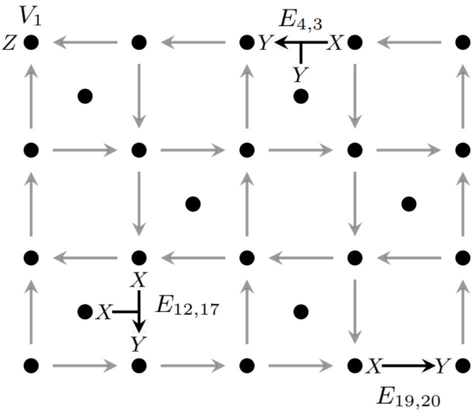

Source: [arXiv:2003.06939]

Physical Subspace

Not every state in the enlarged Hilbert space corresponds to a physical fermionic state.

Physical states satisfy the stabilizer constraints

$$H_{\text{map}} = -\sum \Pi_s \otimes Z_s - \sum \Pi_p \otimes Z_p. \tag{14}$$

For a physical state

$$\langle H_{\text{map}} \rangle = -N_{\text{even}}, \tag{15}$$

where N_{even} denotes the number of even faces.

Hence every loop carries eigenvalue $+1$.

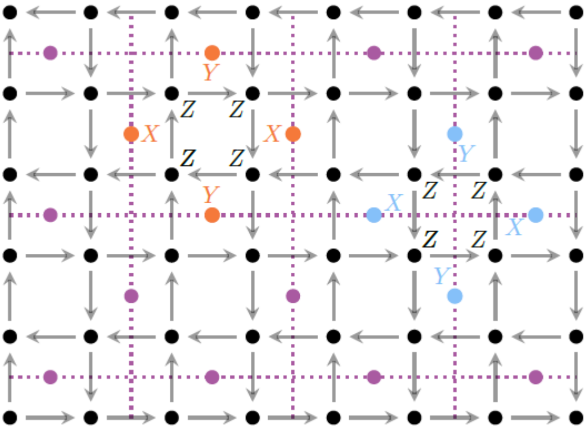

Source: [arXiv:2003.06939]

Penalty Hamiltonian

To suppress nonphysical states, we add a penalty term.

$$H_{\mathrm{modified}} = H + \alpha \left(H_{\mathrm{map}} + N_{\mathrm{even}} \right) . \tag{16}$$

- Penalty term raises the energies of nonphysical states.
- Restricts VQE optimization to the physical sector.
- Choose

$$\alpha > E_n - E_0$$

  to obtain the lowest n eigenstates.

Spinless Hubbard Model

The charge-conjugation symmetric Hamiltonian is

$$H = -J \sum_{\langle ij \rangle} \left(a_i^\dagger a_j + a_j^\dagger a_i \right) \tag{17}$$

$$- \mu \sum_i \left(n_i - \frac{1}{2} \right) + U \sum_{\langle ij \rangle} \left(n_i - \frac{1}{2} \right) \left(n_j - \frac{1}{2} \right). \tag{18}$$

- J : hopping strength.
- μ : chemical potential.
- U : nearest-neighbour interaction.

Local Qubit Hamiltonian

After the DK mapping, the spinless Hubbard model becomes

$$H = -\frac{J}{2}\sum_{\langle ij\rangle}(X_iX_jP_{ij} + Y_iY_jP_{ij}) + \frac{\mu}{2}\sum_i Z_i + \frac{U}{4}\sum_{\langle ij\rangle} Z_iZ_j, \tag{19}$$

where P_{ij} denotes the face-qubit operator associated with edge (i, j).

- The hopping terms remain local even in two dimensions.

Spectrum Validation

The DK mapping enlarges the Hilbert space.

Physical states are selected through stabilizer constraints.

The resulting low-energy spectrum agrees with exact diagonalization.

- QuSpin [SciPost Phys. 7, 020 (2019)]
- Jordan–Wigner [Eur. Phys. J. A 47, 631 (1928).]
- Derby–Klassen [Phys. Rev. B 104, 035118 (2021)]

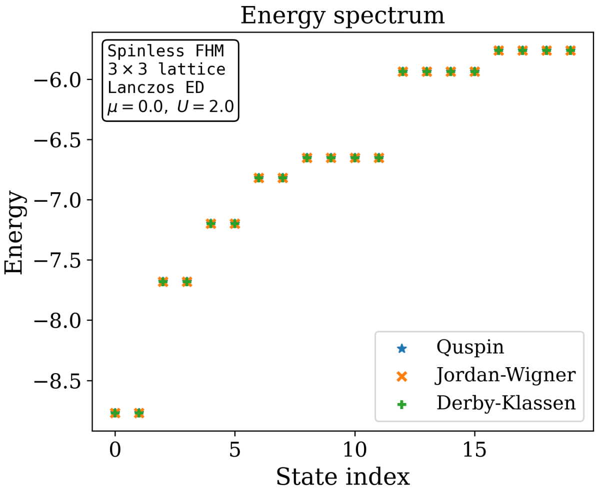

Hamiltonian Variational Ansatz

The ansatz is constructed directly from the Hamiltonian terms:

- Hopping terms
- Interaction terms
- Chemical potential terms

Advantages:

- Physically motivated
- Particle-number conserving
- Reduced search space

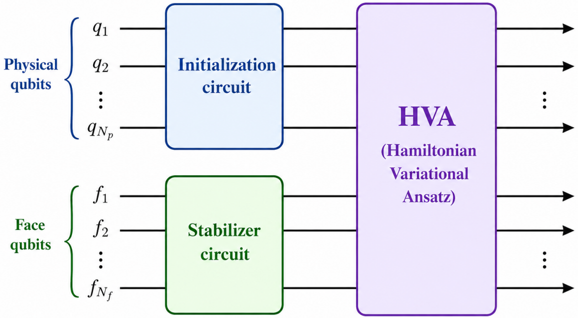

Variational Quantum Deflation (VQD)

Ground-state VQE can be extended to excited states.

The cost function becomes

$$C_n(\theta) = \langle H \rangle_\theta + \sum_{i<n} \beta_i \left| \langle \psi(\theta) | \psi_i \rangle \right|^2 . \tag{20}$$

- Orthogonality is enforced through overlap penalties.
- Ground and excited states are obtained sequentially.
- We compute the lowest three states.

Ground and Excited-State Spectrum

We employ VQE and VQD to compute

- Ground state
- First excited state
- Second excited state

for the 3×3 spinless Hubbard model.

Good agreement with Quspin exact diagonalization is observed.

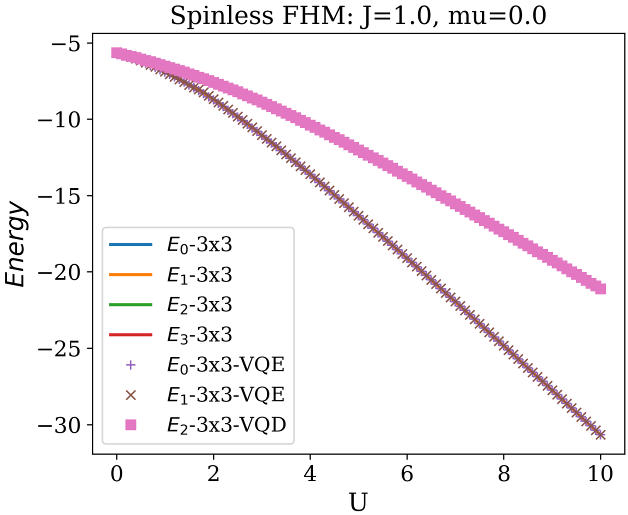

Comparison of JW and DK Mapping

Mapping	Ansatz	layers	Optimizer	E_0(VQE)	Fidelity	Time (min)
JW	SU2-full	8	LBFGS	-8.84520	0.96065	16.3
JW	SU2-linear	8	LBFGS	-8.95076	0.98504	16.6
DK	HVA	8	COBYLA	-8.92192	0.97983	2.3
JW	HVA	8	COBYLA	-8.92617	0.98082	38.4

Table: Single spin FHM 3x3 ($J = 1.0, \mu = 0.5, U = 2.0$,$\mathrm{E}_0 = -9.01941$)

Mapping	Ansatz	layers	Optimizer	E_0(VQE)	Fidelity	Time (hr)
JW	SU2-full	8	COBYLA	-16.3853	0.4504	21.5
JW	SU2-linear	8	COBYLA	-14.3343	0.0003	19.4
DK	HVA	8	COBYLA	-16.2894	0.4384	0.5
JW	HVA	8	COBYLA	-13.38582	0.0049	7.3

Table: Single spin FHM 4x4 (even mapping) ($J = 1.0, \mu = 0.5, U = 2.0, E_0 = -16.8719$)

Resource Estimation

Mapping	Ansatz	parameters	CNOT gates	CNOT depth
JW	SU2-full	$2(N_l+1)L_xL_y$	$2N_lL_xL_y(L_xL_y-1)$	$N_l(L_xL_y+1)$
JW	SU2-linear	$2(N_l+1)L_xL_y$	$N_l(L_xL_y-1)$	$2N_l$
DK	HVA	$N_l(L_xL_y-L_x-L_y+2)$	$10N_l(2L_xL_y-L_x-L_y)+N_S$	$24N_l$
JW	HVA	$N_l(L_xL_y-L_x-L_y+2)$	$N_l(2L_x+4)(2L_xL_y-L_x-L_y)$	$(24+L_x)N_l$

Table: Resource estimation

Tradeoff

- DK mapping introduces auxiliary qubits.
- DK mapping combined with HVA gives comparable performance while preserving locality.
- Circuit depth remains independent of system size.
- Locality is preserved in higher dimensions.

Staggered Occupation and Susceptibility

$$N_{\mathrm{st}} = \sum_r (-1)^r \left(n_r - \frac{1}{2} \right), \qquad \chi = \frac{\langle N_{\mathrm{st}}^2 \rangle}{V}. \tag{21}$$

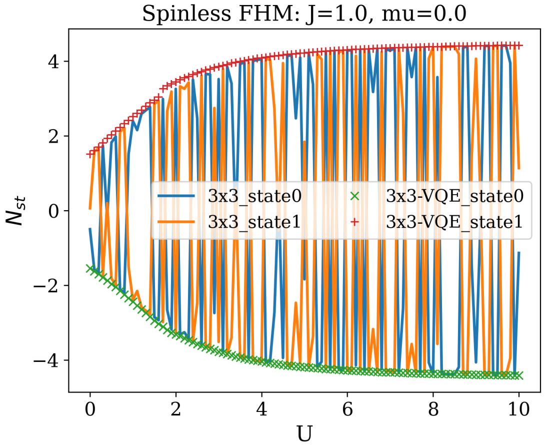

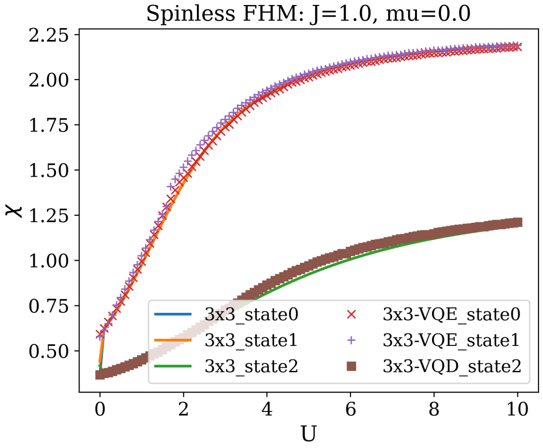

Lifting the Degeneracy

Introducing a small chemical potential lifts the degeneracy, resulting in good agreement between exact diagonalization (ED) and VQE results.

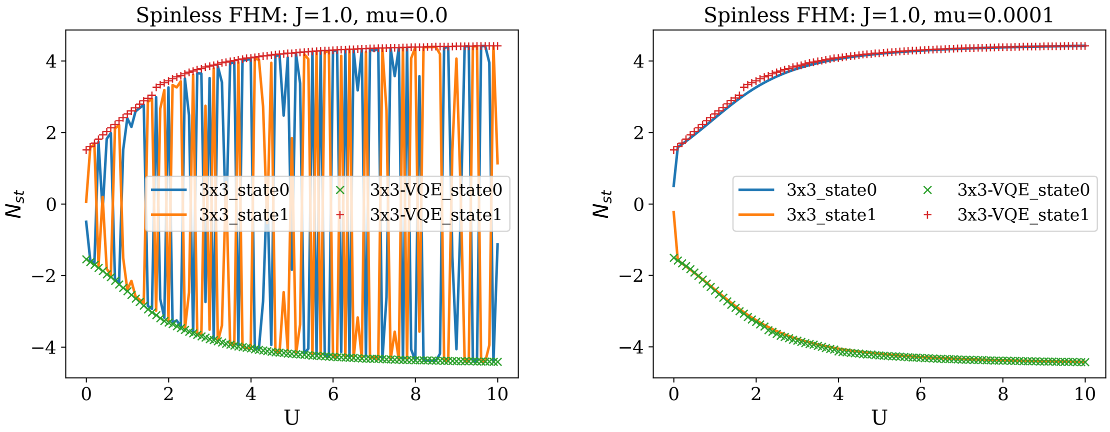

Conclusions

- The Derby–Klassen mapping preserves locality in higher dimensions.
- The Hamiltonian variational ansatz accurately reproduces low-lying spectra and observables.
- Locality preservation enables low-depth HVA circuits with reduced gate overhead.
- Comparison with the Jordan–Wigner mapping demonstrates the advantages of the DK mapping.
- The framework can be readily extended to larger lattices and multi-flavor Fermionic models.

Thank you!

Backup Slides

Simulation Setup

- We have used NVIDIA CUDA-Q (GPU accelerated) backend for exact (noise-free) simulation of state vector.
- Simulations have been done on the **grouse** (NVIDIA-V100) cluster.
- **COBYLA** optimizer has been used.

SU2 full and linear circuits

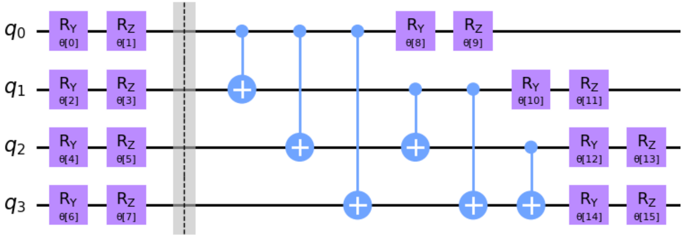

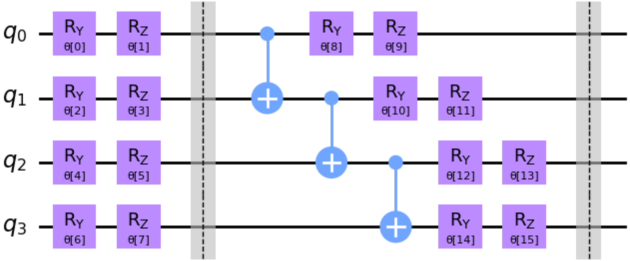

VQE circuit

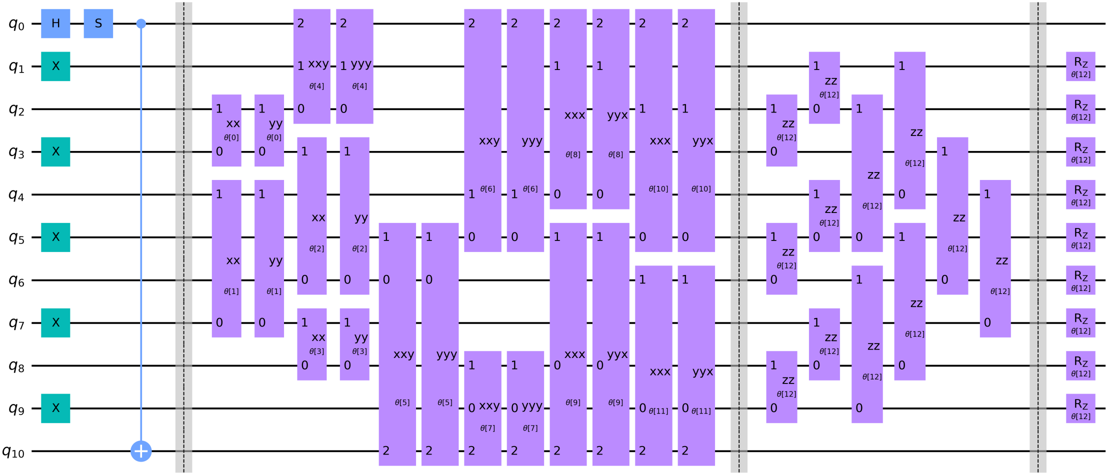

q_0
q_1
q_2
q_3
q_4
q_5
q_6
q_7
q_8
q_9
q_{10}
H
S
X
xx θ[0]
xx θ[1]
yy θ[0]
yy θ[1]
xx θ[2]
xx θ[3]
yy θ[2]
yy θ[3]
xxy θ[4]
yyy θ[4]
xxy θ[5]
yyy θ[5]
xxy θ[6]
yyy θ[6]
xxy θ[7]
yyy θ[7]
xxx θ[8]
yyx θ[8]
xxx θ[9]
yyx θ[9]
xxx θ[10]
yyx θ[10]
xxx θ[11]
yyx θ[11]
zz θ[12]
R_Z θ[12]

Physical condition

Since every nontrivial stabilizer (even-face) is defined by either Pallet or Star Toric code. We can define a map Hamiltonian as,

$$\mathcal{H}_{\text{map}} = -\sum \Pi_s \otimes Z_s - \sum \Pi_p \otimes Z_p. \tag{22}$$

Every loop must have a "+1" eigenvalue for a physical state; all remaining states are non-physical. We can write this condition as,

$$\begin{aligned} \langle\psi| \mathcal{H}_{map} |\psi\rangle &= -1 \times \text{Number of even faces} \\ \implies \langle\psi| (\mathcal{H}_{map} + \text{Number of even faces}) |\psi\rangle &= 0. \end{aligned} \tag{23}$$

where $|\psi\rangle$ is a physical state.

Based on this condition, we can add a penalty term to the Hamiltonian. It adds extra energy to the non-physical states. It forces only the physical state to have low energies.

$$\mathcal{H}_{modified} = \mathcal{H} + \alpha(\mathcal{H}_{map} + \text{Number of even faces}). \tag{24}$$

Where α must be bigger than the energy spectrum we want to calculate. Say we want to calculate n energy states, then $\alpha > (E_n - E_0)$.

Simulate the heavy tetraquark

$$bb\bar{u}\bar{d}$$

using the Hamiltonian

$$H = \sum_i \left(m_i - \frac{\hbar^2}{2m_i}\nabla^2 \right) + \sum_{i<j} \left(V_{\mathrm{CON}}(r_{ij}) + V_{\mathrm{OGE}}(r_{ij}) \right).$$

- Particle picture
- Qubitized color interactions
- Trotter evolution
- Variational Quantum Eigensolver

Qubitized Gell-Mann Operators

$$\lambda_1 = \frac{1}{2}\sigma_2^x + \frac{1}{2}\sigma_1^z\sigma_2^x \qquad \lambda_2 = \frac{1}{2}\sigma_2^y + \frac{1}{2}\sigma_1^z\sigma_2^y$$

$$\lambda_3 = \frac{1}{2}\sigma_2^z + \frac{1}{2}\sigma_1^z\sigma_2^z \qquad \lambda_4 = \frac{1}{2}\sigma_1^x + \frac{1}{2}\sigma_1^x\sigma_2^z$$

$$\lambda_5 = \frac{1}{2}\sigma_1^y + \frac{1}{2}\sigma_1^y\sigma_2^z$$

$$\lambda_6 = \frac{1}{2}\sigma_1^x\sigma_2^x + \frac{1}{2}\sigma_1^y\sigma_2^y$$

$$\lambda_7 = -\frac{1}{2}\sigma_1^x\sigma_2^y + \frac{1}{2}\sigma_1^y\sigma_2^x$$

$$\lambda_8 = \frac{1}{\sqrt{3}}\sigma_1^z - \frac{1}{2\sqrt{3}}\sigma_2^z + \frac{1}{2\sqrt{3}}\sigma_1^z\sigma_2^z$$

Particle Picture

- Heavy quarks:

$$\text{color} \otimes \text{spin}$$

- Light quarks:

$$\text{color} \otimes \text{spin} \otimes \text{space}$$

- Color interactions:

$$\vec{\lambda} \cdot \vec{\lambda}, \qquad \vec{\lambda} \cdot \vec{\lambda}^*$$

Degree of Freedom	Qubits
Color	2
Spin	1
Space	2

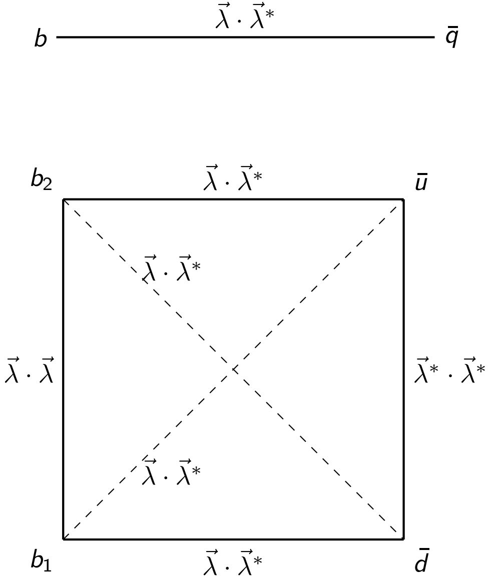

Variational Quantum Eigensolver

- EfficientSU2 ansatz with 12 layers
- Comparison with Exact Diagonalization

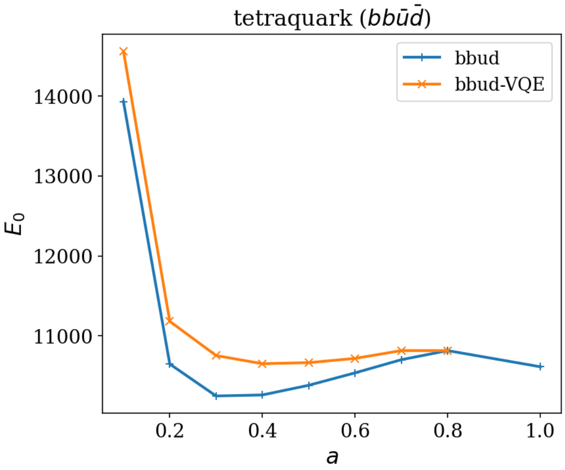

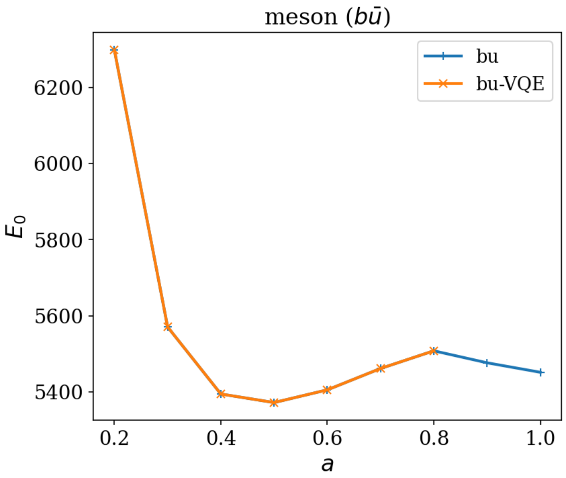

Degeneracy and Penalty Terms

Ground state of the meson has four-fold degeneracy:

- One spin singlet
- Three spin triplets

Spin-singlet sector:

$$H_{\text{singlet}} = H + \alpha\left(\vec{\sigma}_b \cdot \vec{\sigma}_{\bar{u}} + 3\right)$$

Spin-triplet sector:

$$H_{\text{triplet}} = H - \alpha\left(\vec{\sigma}_b \cdot \vec{\sigma}_{\bar{u}} - 1\right)$$

Outlook

- Than *et al.* [arXiv:2501.00579] employed the Kogut–Susskind Hamiltonian formulation to study the one-dimensional QCD phase transition on quantum hardware.
- Alternative approaches, such as the Quantum Link Model [hep-lat/9609042] and the Loop-String-Hadron formulation [arXiv:1912.06133], provide qubit-based Hamiltonians, although their extension to higher dimensions remains under active investigation.
- Alongside the variational quantum eigensolver (VQE) [arXiv:1304.3061], several hybrid quantum-classical algorithms, including the quantum approximate optimization algorithm (QAOA) [arXiv:1411.4028], sample-based quantum diagonalization (SQD) [arXiv:2405.05068], and sample-based Krylov quantum diagonalization (SKQD) [arXiv:2501.09702], have emerged as promising approaches for achieving quantum utility.